JACS
JOURNAL OF THE AMERICAN CHEMICAL SOCIETY
pubs.acs.org/JACS

Article

Metallaantiaromaticity of 10-Platinacorrole Complexes

Kazuki Miwa, Tomoya Yokota, Qian Wang, Takahiro Sakurai, Heike Fliegl, Dage Sundholm,* and Hiroshi Shinokubo*

Cite This: J. Am. Chem. Soc. 2024, 146, 1396−1402

Read Online

ACCESS | Metrics & More | Article Recommendations | Supporting Information

ABSTRACT: The aromaticity of cyclic π-conjugated organometallic compounds is known as metallaaromaticity. π-Conjugated metallacycles, such as metallabenzenes and metallapentalenes, have been investigated in order to understand the involvement of the d electrons from the metal center in the π-conjugated systems of the organic ligands. Here, we report the synthesis of Pd(II) 10-platinacorrole complexes with cyclooctadiene (COD) and norbornadiene (NBD) ligands. While the Pd(II) 10-platinacorrole COD complex adopts a distorted structure without showing appreciable antiaromaticity, the corresponding NBD complex exhibits a distinct antiaromatic character due to its highly planar conformation. Detailed density functional theory (DFT) calculations revealed that two d orbitals are involved in macrocyclic π-conjugation. We furthermore demonstrated that Craig−Möbius antiaromaticity is not present in the studied system. The synthesis of 10-platinacorroles enables a systematic comparison of the antiaromaticity and aromaticity of closely related porphyrin analogues, providing a better understanding of π-conjugation that involves d orbitals.

INTRODUCTION

Aromaticity is a fundamental concept in chemistry and is usually observed in planar cyclic π-conjugated organic molecules. However, various new types of nonclassical aromaticity have been proposed and researched intensively.[1−7] One such type is metallaaromaticity, which has been defined as the aromatic properties of organometallacycles that consist of a σ-bonded transition metal and π-conjugated organic ligand.[8−11] The discovery of metallabenzenes[12−14] and metallapentalenes[15−17] has opened up new avenues for the exploration and understanding of the electronic structure and the bonding nature of organometallic compounds (Figure 1a). However, metallaaromaticity has hitherto only been achieved in relatively small ring systems and examples of macrocyclic metallaaromatic molecules remain limited.[18,19]

Owing to the specific shape of the d orbitals, topological issues arise in the molecular orbitals of π-conjugated metallacycles. The conjugation of the d_{zx} orbital of the metal center with the p_z orbital of a ligand enables Hückel aromaticity in planar cyclic π-conjugated systems with $4n + 2$ (n = 0, 1, 2, ...) π-electrons (Figure 1b). In contrast, participation of the d_{yz} orbital in the π-conjugated system

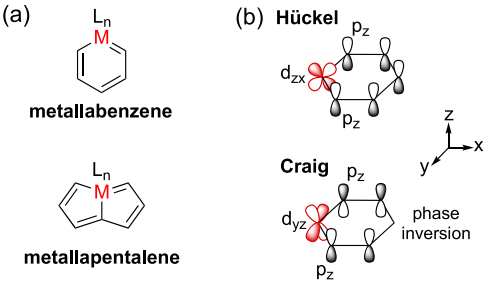

Figure 1. (a) Metallabenzenes and metallapentalenes. (b) Involvement of the d_{zx} and d_{yz} orbitals in π-conjugated systems.

results in a phase inversion of the molecular orbital, thus inducing Craig−Möbius antiaromaticity with $4n + 2$ (n = 0, 1,

Received: September 18, 2023
Revised: December 20, 2023
Accepted: December 21, 2023
Published: January 3, 2024

https://doi.org/10.1021/jacs.3c10250
J. Am. Chem. Soc. 2024, 146, 1396−1402

2, ...) π-electrons.[20] Consequently, the aromaticity of metallacycles can be complicated when two d orbitals are involved in a cyclic π-conjugated system.[21]

Porphyrins and other related molecules, namely, porphyrinoids, are examples of macrocyclic π-conjugated systems. The aromaticity of various porphyrinoids has been actively investigated.[22−25] Porphyrinoids are excellent scaffolds for achieving effective macrocyclic π-conjugation, thus enabling aromaticity in Möbius π-systems,[26,27] large macrocycles,[28] and macrocycles that contain metallocene units.[29−31] Among various porphyrinoids, the macrocyclic aromaticity and antiaromaticity of 10-heterocorroles are sensitive to the heteroatoms incorporated at the 10-position, thus highlighting the important role that the heteroatoms play in the cyclic conjugation (Figure 2).[32−34] While a lone pair on either

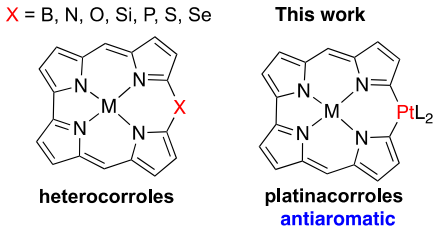

Figure 2. Structures of 10-heterocorroles and 10-platinacorrole.

nitrogen (X = N),[35,36] oxygen (X = O),[37,38] sulfur (X = S),[38,39] phosphorus (X = P),[40] or selenium (X = Se)[38] in conjunction with the 16π-conjugation of the bis(dipyrrin) unit leads to macrocyclic 18π-conjugated aromatic systems, 10-boracorrole (X = B)[41] exhibits a unique form of global antiaromaticity due to the vacant p orbital on the boron atom, which affords a 16π-conjugated system. 10-Silacorrole (X = Si)[42] shows no global antiaromaticity because the sp^3-hybridized silicon atom disrupts the macrocyclic π-conjugation. In other words, the global aromaticity or antiaromaticity of 10-heterocorroles depends on the degree of π-conjugation that manifests via the heteroatom linkage.

In this context, 10-metallacorroles should offer an ideal molecular scaffold for the systematic evaluation of the macrocyclic π-conjugation that occurs through metal−carbon bonds via the d orbitals. If π-electrons can be delocalized through the transition metal at the 10-position, the molecule should show either metallaaromaticity or metallaantiaromaticity. Here, we report the synthesis of two Pd(II) 10-platinacorrole complexes and their ligand-dependent antiaromaticity. 10-Platinacorrole is a molecular entity that significantly expands the scope of metallaaromaticity because this molecule demonstrates that metallaaromaticity can manifest in macrocyclic π-conjugated systems such as porphyrinoids.

RESULTS AND DISCUSSION

Synthesis, Structure, and Aromaticity of a Pd(II) 10-Platinacorrole COD Complex. The synthesis of the Pd(II) 10-platinacorrole complex started from dibromobis(dipyrrin) **1** (Scheme 1a). The palladium-catalyzed Miyaura−Ishiyama borylation of **1** afforded the corresponding diborylated bis(dipyrrin) **2** in 63% yield.[43] Subsequently, **2** was metalated with a Pd(II) ion to fix the conformation of the two boryl groups on the same side. Transmetalation of Pd(II) bis(dipyrrin) **3** with dichloro(1,5-cyclooctadiene)platinum(II)

Scheme 1. Synthesis of Pd(II) 10-Platinacorrole COD Complex 4

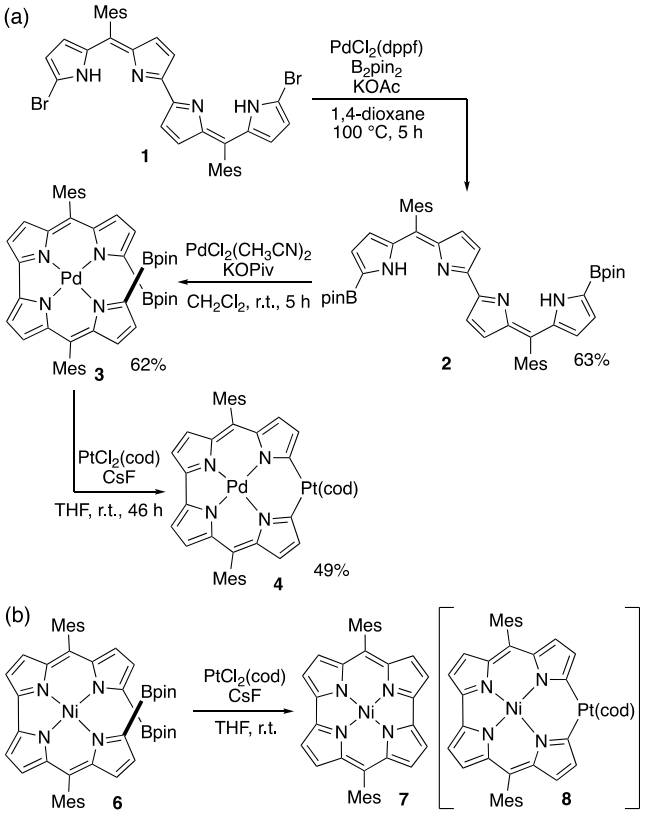

furnished Pd(II) 10-platinacorrole cyclooctadiene (COD) complex **4** in 49% yield.[44] Platinacorrole **4** was structurally characterized by ^{1}H, ^{13}C, and ^{195}Pt NMR spectroscopy, as well as high-resolution mass spectrometry. Notably, metalation with palladium is essential for the successful isolation of **4** (Scheme 1b). A similar transmetalation of Ni(II) bis(dipyrrin) **6** with the same platinum salt used in the synthesis of **4** resulted in the formation of Ni(II) norcorrole **7**. This probably occurs via the reductive elimination of platinacorrole **8**, which is most likely due to the fact that the ionic radius of Ni(II) (0.49 Å) is smaller than that of Pd(II) (0.64 Å).[45]

The ^{1}H NMR spectrum of 10-platinacorrole COD complex **4** contains resonances for the pyrrole protons between 6.2 and 5.9 ppm, which are slightly upfield shifted compared to those of Pd(II) bis(dipyrrin) complex **5**, which does not exhibit any macrocyclic π-conjugation (Figure 3a,b). The molecular structure of **4** was unambiguously determined via single-crystal X-ray diffraction analysis (Figure 4a,b). The molecular skeleton of **4** is significantly distorted, and the Pt(II) center protrudes from the tetrapyrrole moiety. The Pt(II) center is displaced by 1.09 Å from the mean plane, which is defined by the 24 core atoms consisting of the four pyrrole units, the *meso*-carbon atoms, the palladium atom, and the platinum atom. The distance between the Pt(II) and Pd(II) centers of **4** is 3.738 Å.

We then evaluated the aromatic nature of platinacorrole COD complex **4** by using density functional theory (DFT) calculations. The optimized structure of **4** by the DFT calculation using the B3LYP functional[46] and def2-TZVP basis set[47] reproduced nicely its experimental structure (Figures 4c and S30). The aromaticity of **4** was examined in terms of its magnetic criteria using nucleus independent chemical shift (NICS) analysis.[48] Judging from the marginally

https://doi.org/10.1021/jacs.3c10250
J. Am. Chem. Soc. 2024, 146, 1396−1402

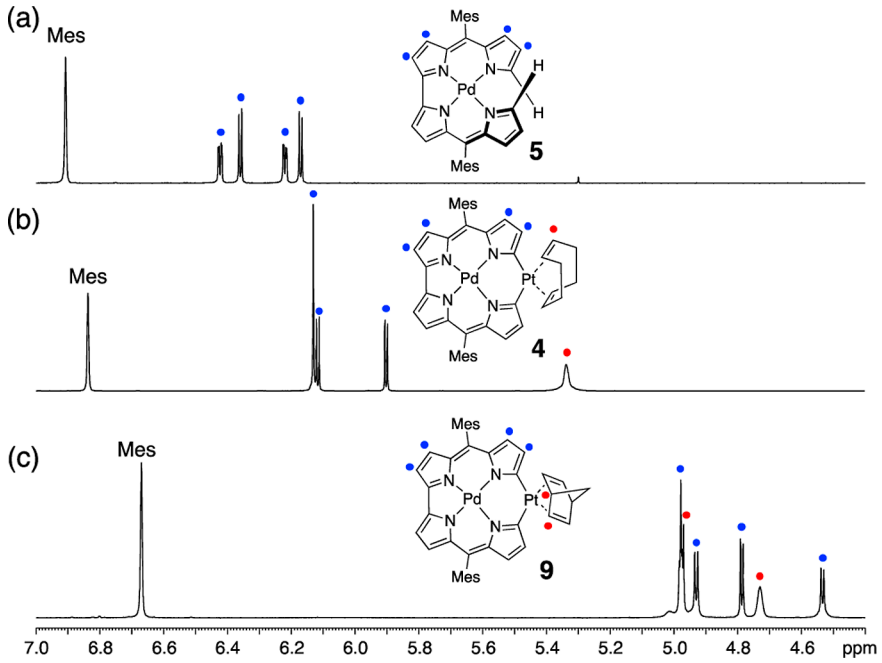

Figure 3. ^{1}H NMR spectra of (a) bis(dipyrrin) **5**, (b) the COD complex **4**, and (c) the NBD complex **9** in $CDCl_3$.

positive NICS(1) values of about +3 ppm, we concluded that COD complex **4** is nonaromatic (Figure S34). Clearly, the nonplanar structure of **4** interrupts the effective electronic conjugation through the C−Pt−C linkage, resulting in it being nonaromatic. Current-density calculations using the GIMIC program[49−55] support this conclusion (vide infra).

Synthesis, Structure, and Aromaticity of Pd(II) 10-Platinacorrole Norbornadiene (NBD) Complex 9. The deformed structure of **4** most likely arises from steric repulsion between the COD ligand and adjacent pyrrole subunits. We therefore expected that exchange of the COD ligand to a sterically less demanding NBD ligand would allow planarization of the core skeleton. Treatment of **4** with a large excess of NBD in acetone resulted in the precipitation of the 10-platinacorrole NBD complex **9** in 58% yield (Scheme 2).

The planar structure of NBD complex **9** was confirmed by single-crystal X-ray diffraction analysis and DFT calculations. Figure 4d,e shows the crystal structure of **9**, of which the crystal was obtained from octane/chlorobenzene. The mean plane deviation of **9** is 0.098 Å, which is substantially smaller than that of **4** (0.229 Å), and the Pt(II) atom protrudes by merely 0.482 Å from the mean plane. The supplementary crystal structure of **9** obtained from octane/chloroform adopts a more planar conformation (Figure S28). The slightly distorted structure of **9** is likely due to crystal packing forces induced by its dimeric packing arrangement (Figure S27). The optimized structure of **9** at the B3LYP/def2-TZVP level starting from the nonplanar geometry without any restriction resulted in a perfectly planar conformation belonging to the C_{2v} point group (Figures 4f and S31). We also simulated the conformation of 10-platinacorrole with ethylene, 1,3-butadiene, and acetonitrile ligands, none of which afforded a planar structure (Figure S33). This result suggests that a bidentate and less-hindered ligand is essential to planarizing the structure of **9**.

The planar conformation of NBD complex **9** allows for overlap between the d orbitals on the Pt center and the p orbitals on the adjacent carbon atoms, thus enabling effective macrocyclic π-conjugation through the platinum center. In the ^{1}H NMR spectrum of **9**, the pyrrole protons (4.5−5.0 ppm) were substantially upfield shifted relative to those of **4**, suggesting the presence of a paratropic ring-current effect (Figure 3c). The ^{1}H NMR spectra of **9** at low temperatures exhibited further upfield shifts of pyrrole protons, suggesting its planar and dynamic conformation (Figure S18). The unique antiaromaticity of **9** was confirmed based on its magnetic properties using NICS(1) calculations at the BHLYP/def2-TZVP level. The calculated NICS(1) values range from 8.4 to 11.5 ppm (Figure S35). A substantial paratropic ring current was confirmed using the GIMIC method (vide infra).[49−55] The ring current effect of **9** was compared with that of other Pd(II) 10-heterocorroles. NICS(1) calculations clarify the aromaticity, nonaromaticity, and antiaromaticity of 10-thia-, 10-sila-, and 10-boracorroles, respectively, according to magnetic criteria (Figures S36−S38). Compared with distinctly antiaromatic Pd(II) boracorrole, of which NICS(1) values range from 16.6 to 21.0 ppm, the paratropicity of **9** is attenuated. The effect of the central metal was also investigated. Ni(II) and Zn(II) 10-platinacorrole NBD complexes exhibit comparable antiaromaticity judging from their NICS(1) values (Figures S39 and S40).

Optical and Electrochemical Properties of Pd(II) 10-Platinacorroles 4 and 9. The conformational difference between platinacorroles **4** and **9** significantly influences the gap between their highest occupied (HOMOs) and lowest unoccupied molecular orbitals (LUMOs), thus resulting in substantial differences in their optical and electrochemical properties. The UV/vis/NIR absorption spectra of COD complex **4** exhibits a broad absorption band from 700 to 1000 nm (Figure 5). The spectral shape is similar to that of the corresponding 10-silacorrole, which also lacks macrocyclic π-conjugation.[42] In contrast, broad and weak absorption bands tailing to 1500 nm were observed for NBD complex **9**. This feature arises from the forbidden HOMO → LUMO transition, which is typical for antiaromatic porphyrinoids.[56] Time-dependent DFT (TD-DFT) calculations[57] at the CAM-

https://doi.org/10.1021/jacs.3c10250
J. Am. Chem. Soc. 2024, 146, 1396−1402

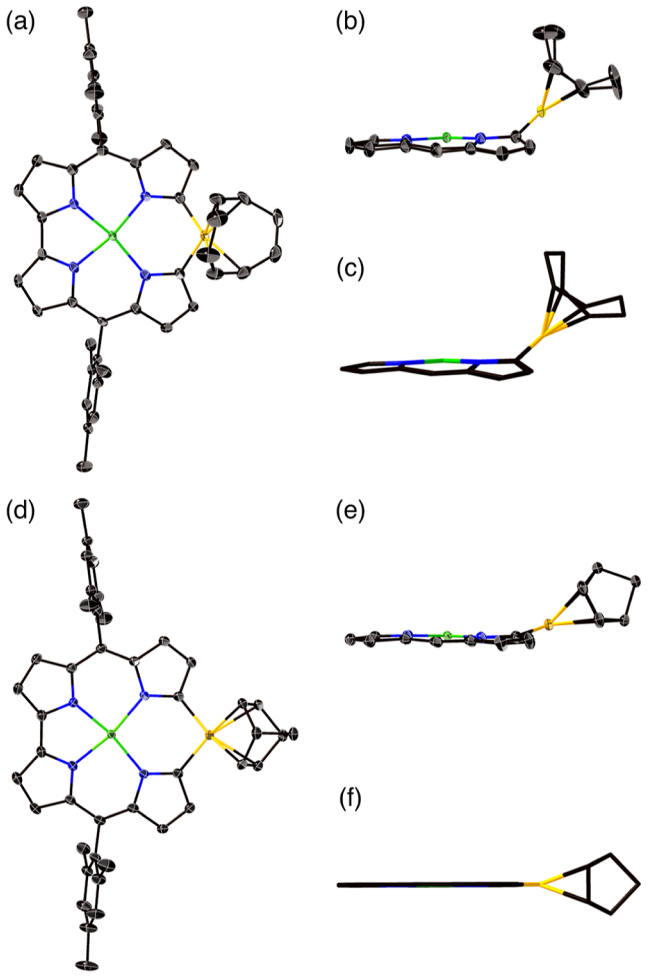

Figure 4. (a) Top and (b) side views of the X-ray crystal structure of **4**. (c) Side view of the optimized structure of **4** at the B3LYP/def2-TZVP level. (d) Top and (e) side views of the X-ray crystal structure of **9**. (f) Side view of the optimized structure of **9** at the B3LYP/def2-TZVP level. Hydrogen atoms and mesityl substituents except in parts (a,d) are omitted for clarity.

Scheme 2. Synthesis of Pd(II) 10-Platinacorrole NBD Complex 9

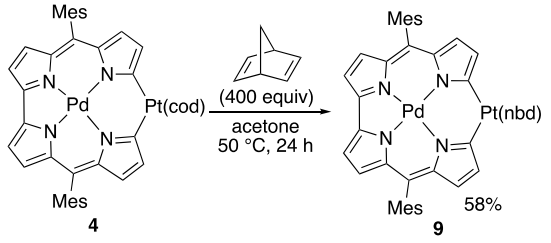

B3LYP[58]/def2-TZVP level for **4** and **9** were able to reproduce their experimental absorption spectra, in which the NIR absorption bands were assigned as HOMO → LUMO transitions (Figure S42; Table S2).

The electrochemistry of platinacorroles **4** and **9** was investigated by using cyclic voltammetry (Figure S29). NBD complex **9** exhibited two reversible oxidation waves at −0.04 and 0.54 V as well as two reversible reduction waves at −1.35 and −1.87 V. Notably, the electrochemical HOMO−LUMO gap of **9** (1.31 V) is substantially narrower than that of COD complex **4** (1.68 V). This observation is consistent with the results of the DFT calculations. A small HOMO−LUMO gap is also typical for antiaromatic porphyrinoids.

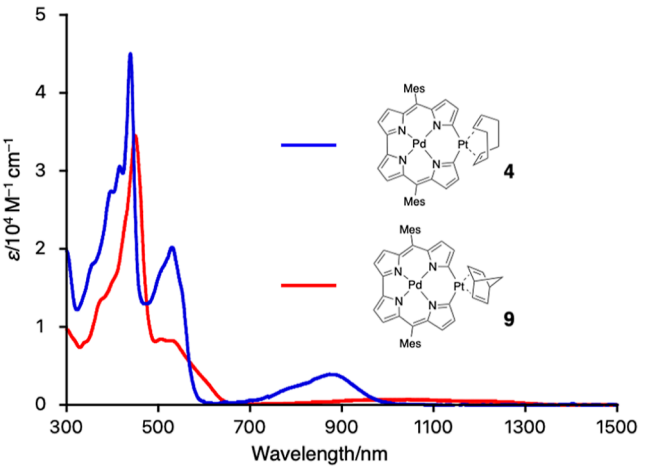

Figure 5. UV/vis/NIR absorption spectra of **4** and **9** in dichloromethane.

Ring-Current Analysis and Origin of the Antiaromaticity in Platinacorrole Complexes. The ring current in platinacorrole complexes **4** and **9** was visualized and quantified via current-density studies using the GIMIC method.[49−55] The calculations were performed on simplified models **4′** and **9′**, where the mesityl groups are replaced by hydrogen atoms. The current-density calculations demonstrate that **9′** features global antiaromaticity with many current-density pathways (Figure 6a). While a very weak paratropic ring current of −1.7 nA T^{-1}

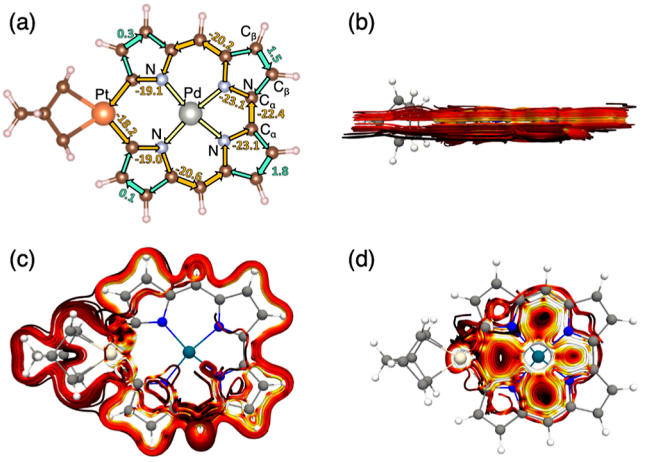

Figure 6. (a) GIMIC analysis of NBD complex **9′** calculated at the B3LYP/def2-TZVP level. The integrated ring-current strength susceptibilities across the selected bonds are shown in nA T^{-1}. (b) Side view of the current density. (c) The diatropic current-density contribution. (d) The paratropic current-density contribution.

passes though the Pt−C bond of the COD complex **4′** (Figure S43), NBD complex **9′** exhibits a substantial paratropic ring current of −18.2 nA T^{-1} at the Pt−C bond, highlighting its antiaromaticity. A paratropic ring current of −22.4 nA T^{-1} flows through the C_α−C_α linkage and mainly circulates along the inner pathway at each pyrrole ring. This feature is typical for antiaromatic porphyrinoids.[25] Part of the paratropic ring current (9−10 nA T^{-1}) is diverted via the Pd atom. In addition, a weak diatropic edge current of approximately 2 nA

https://doi.org/10.1021/jacs.3c10250
J. Am. Chem. Soc. 2024, 146, 1396−1402

T^{-1} flows through the C_β−C_β bonds. The diatropic and paratropic contributions to the ring current are shown in Figure 6c,d, respectively. Importantly, the current-density flow stays on the same side of the molecular plane (Figure 6b). If Craig−Möbius antiaromaticity applies to the present system, a ring-current associated with a phase inversion of the molecular orbitals (MOs) would be expected. The visualization of the ring current indicates that Craig−Möbius antiaromaticity is not applicable to the platinacorrole complexes studied here.

Thus, to understand the origin of the antiaromatic nature of 10-platinacorrole NBD complex **9**, we examined the molecular orbitals of simplified model **9′** (Figure S41). In several MOs, the d orbitals on the Pt center are effectively overlapped with the π orbitals of the tetrapyrrole unit (Figure 7a). The natural

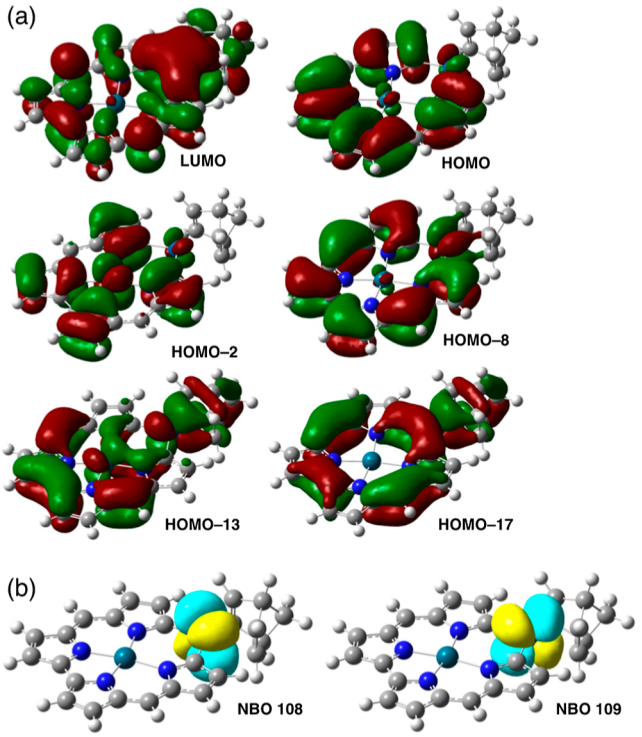

Figure 7. (a) Selected MOs of **9′**. (b) NBOs for the d_{zx} and d_{yz} orbitals of **9′**. Calculations were performed at the B3LYP/def2-TZVP level (isovalue: 0.02).

bond orbital (NBO) analysis of these MOs reveals large contribution from NBOs 109 and 108, which correspond to the d_{zx} and d_{yz} orbitals of the Pt center (Figure 7b).[59] The Pt(II) center adopts a square-planar geometry with a formal d^8 electronic configuration. Of the four occupied d orbitals, only the d_{yz} and d_{zx} orbitals participate in the π-conjugation because the π MOs should be antisymmetric relative to the molecular plane (Figure 8). Consequently, four d electrons from the Pt(II) center of NBD complex **9** are involved in the π-

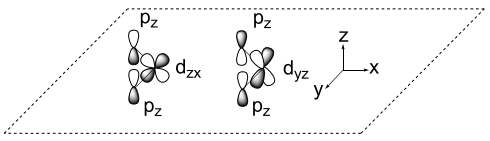

Figure 8. π-Conjugation involving d_{zx} and d_{yz} orbitals.

conjugation along the inner pathway, thus formally creating a cyclic 20π-conjugated system.

CONCLUSIONS

We synthesized Pd(II) 10-platinacorrole COD and NBD complexes **4** and **9**, respectively. Single-crystal X-ray diffraction analyses and density functional theory (DFT) calculations confirmed nonplanar and planar structures for the COD complex **4** and NBD complex **9**, respectively. The planar conformation of **9** induces an effective overlap of the $5d_{yz}$ and $5d_{zx}$ orbitals of the platinum center with the $2p_z$ orbitals of the adjacent carbon atoms. The effective π-conjugation through the Pt center results in the distinct antiaromatic character of **9**. This notion was supported by an examination of the magnetic properties of **9** using spectroscopic analyses and DFT calculations, which revealed a distinct paratropic ring-current effect and a narrow HOMO−LUMO gap. A detailed evaluation of the ring currents in **9** using the GIMIC method demonstrated that Craig−Möbius antiaromaticity is not present in this system. Thus, 10-platinacorrole complex **9** showcases that metallaantiaromaticity is possible in macrocyclic π-conjugated systems, thus offering a better understanding of π-conjugation through d orbitals and expanding the research field of metallaaromaticity.

ASSOCIATED CONTENT

Supporting Information

The Supporting Information is available free of charge at https://pubs.acs.org/doi/10.1021/jacs.3c10250.

Experimental procedures, NMR spectra, mass spectra, additional experimental details, and details of calculations (PDF)

Accession Codes

CCDC 2309448−2309449 contain the supplementary crystallographic data for this paper. These data can be obtained free of charge via www.ccdc.cam.ac.uk/data_request/cif, or by emailing data_request@ccdc.cam.ac.uk, or by contacting The Cambridge Crystallographic Data Centre, 12 Union Road, Cambridge CB2 1EZ, UK; fax: +44 1223 336033.

AUTHOR INFORMATION

Corresponding Authors

Dage Sundholm − *Department of Chemistry, Faculty of Science, University of Helsinki, FIN-00014 Helsinki, Finland;* orcid.org/0000-0002-2367-9277; Email: sundholm@chem.helsinki.fi

Hiroshi Shinokubo − *Department of Molecular and Macromolecular Chemistry, Graduate School of Engineering and Integrated Research Consortium on Chemical Sciences (IRCCS), Nagoya University, Nagoya 464-8603 Aichi, Japan;* orcid.org/0000-0002-5321-2205; Email: hshino@chembio.nagoya-u.ac.jp

Authors

Kazuki Miwa − *Department of Molecular and Macromolecular Chemistry, Graduate School of Engineering and Integrated Research Consortium on Chemical Sciences (IRCCS), Nagoya University, Nagoya 464-8603 Aichi, Japan*

Tomoya Yokota − *Department of Molecular and Macromolecular Chemistry, Graduate School of Engineering and Integrated Research Consortium on Chemical Sciences*

https://doi.org/10.1021/jacs.3c10250
J. Am. Chem. Soc. 2024, 146, 1396−1402

(IRCCS), Nagoya University, Nagoya 464-8603 Aichi, Japan

Qian Wang − *Department of Chemistry, Faculty of Science, University of Helsinki, FIN-00014 Helsinki, Finland*

Takahiro Sakurai − *Department of Molecular and Macromolecular Chemistry, Graduate School of Engineering and Integrated Research Consortium on Chemical Sciences (IRCCS), Nagoya University, Nagoya 464-8603 Aichi, Japan*

Heike Fliegl − *FIZ Karlsruhe—Leibniz Institute for Information Infrastructure, 76344 Eggenstein-Leopoldshafen, Germany*

Complete contact information is available at: https://pubs.acs.org/10.1021/jacs.3c10250

Notes

The authors declare no competing financial interest.

■ ACKNOWLEDGMENTS

This work was supported by JSPS KAKENHI grants JP20H05862, JP20H05863, JP22H04974, and JP22K19025. T.S. expresses his gratitude for a JSPS Research Fellowship for Young Scientists (JP23KJ1073). The authors thank Prof. Norihito Fukui and Dr. Ryo Nakano (Nagoya University) for their help with X-ray diffraction analyses. The research has been also supported by The Academy of Finland through project 340583. Q.W. acknowledges the China Scholarship Council for a predoctoral fellowship. The Finnish IT Center for Science is gratefully acknowledged for computer time.

■ REFERENCES

(1) Merino, G.; Solà, M.; Fernández, I.; Foroutan-Nejad, C.; Lazzeretti, P.; Frenking, G.; Anderson, H. L.; Sundholm, D.; Cossío, F. P.; Petrukhina, M. A.; Wu, J.; Wu, J. I.; Restrepo, A. Aromaticity: Quo Vadis. *Chem. Sci.* **2023**, *14*, 5569−5576.

(2) Schleyer, P. v. R. Introduction: Aromaticity. *Chem. Rev.* **2001**, *101*, 1115−1118.

(3) Stanger, A. What Is . . . Aromaticity: A Critique of the Concept of Aromaticity—Can It Really Be Defined? *Chem. Commun.* **2009**, 1939−1947.

(4) Hoffmann, R. The Many Guises of Aromaticity. *Am. Sci.* **2015**, *103*, 18.

(5) Solà, M. Aromaticity Rules. *Nat. Chem.* **2022**, *14*, 585−590.

(6) El Bakouri, O.; Szczepanik, D. W.; Jorner, K.; Ayub, R.; Bultinck, P.; Solà, M.; Ottosson, H. Three-Dimensional Fully π-Conjugated Macrocycles: When 3D-Aromatic and When 2D-Aromatic-in-3D? *J. Am. Chem. Soc.* **2022**, *144*, 8560−8575.

(7) Schleyer, P. v. R.; Jiao, H. What is aromaticity? *Pure Appl. Chem.* **1996**, *68*, 209−218.

(8) Chen, D.; Hua, Y.; Xia, H. Metallaaromatic Chemistry: History and Development. *Chem. Rev.* **2020**, *120*, 12994−13086.

(9) Fernández, I.; Frenking, G.; Merino, G. Aromaticity of Metallabenzenes and Related Compounds. *Chem. Soc. Rev.* **2015**, *44*, 6452−6463.

(10) Zhu, J. Open Questions on Aromaticity in Organometallics. *Commun. Chem.* **2020**, *3*, 161.

(11) Chen, J.; Jia, G. Recent Development in the Chemistry of Transition Metal-Containing Metallabenzenes and Metallabenzynes. *Coord. Chem. Rev.* **2013**, *257*, 2491−2521.

(12) Bleeke, J. R. Metallabenzenes. *Chem. Rev.* **2001**, *101*, 1205−1228.

(13) Wright, L. J. Metallabenzenes and Metallabenzenoids. *Dalton Trans.* **2006**, 1821−1827.

(14) Landorf, C. W.; Haley, M. M. Recent Advances in Metallabenzene Chemistry. *Angew. Chem., Int. Ed.* **2006**, *45*, 3914−3936.

(15) Zhu, C.; Xia, H. Carbolong Chemistry: A Story of Carbon Chain Ligands and Transition Metals. *Acc. Chem. Res.* **2018**, *51*, 1691−1700.

(16) Zhu, C.; Li, S.; Luo, M.; Zhou, X.; Niu, Y.; Lin, M.; Zhu, J.; Cao, Z.; Lu, X.; Wen, T.; Xie, Z.; Schleyer, P. v. R.; Xia, H. Stabilization of Anti-Aromatic and Strained Five-Membered Rings with a Transition Metal. *Nat. Chem.* **2013**, *5*, 698−703.

(17) Zhu, C.; Luo, M.; Zhu, Q.; Zhu, J.; Schleyer, P. v. R.; Wu, J. I.-C.; Lu, X.; Xia, H. Planar Möbius Aromatic Pentalenes Incorporating 16 and 18 Valence Electron Osmiums. *Nat. Commun.* **2014**, *5*, 3265.

(18) Wei, J.; Zhang, Y.; Chi, Y.; Liu, L.; Zhang, W.-X.; Xi, Z. Aromatic Dicupra[10]Annulenes. *J. Am. Chem. Soc.* **2016**, *138*, 60−63.

(19) An, K.; Shen, T.; Zhu, J. Craig-Type Möbius Aromaticity and Antiaromaticity in Dimetalla[10]Annulenes: A Metal-Induced Yin-and-Yang Pair. *Organometallics* **2017**, *36*, 3199−3204.

(20) Craig, D. P.; Paddock, N. L. A Novel Type of Aromaticity. *Nature* **1958**, *181*, 1052−1053.

(21) Szczepanik, D. W.; Solà, M. Electron Delocalization in Planar Metallacycles: Hückel or Möbius Aromatic? *ChemistryOpen* **2019**, *8*, 219−227.

(22) Osuka, A.; Saito, S. Expanded Porphyrins and Aromaticity. *Chem. Commun.* **2011**, *47*, 4330−4339.

(23) Saito, S.; Osuka, A. Expanded Porphyrins: Intriguing Structures, Electronic Properties, and Reactivities. *Angew. Chem., Int. Ed.* **2011**, *50*, 4342−4373.

(24) Stępień, M.; Sprutta, N.; Latos-Grażyński, L. Figure Eights, Möbius Bands, and More: Conformation and Aromaticity of Porphyrinoids. *Angew. Chem., Int. Ed.* **2011**, *50*, 4288−4340.

(25) Sundholm, D.; Fliegl, H. Aromatic Pathways in Porphyrinoids by Magnetically Induced Ring Currents. In *Handbook of Porphyrin Science*; Kadish, K. M., Smith, K. M., Guilard, R., Eds.; World Scientific, 2022; Vol. *46*, pp 1−39.

(26) Stępień, M.; Latos-Grażyński, L.; Sprutta, N.; Chwalisz, P.; Szterenberg, L. Expanded Porphyrin with a Split Personality: A Hückel-Möbius Aromaticity Switch. *Angew. Chem., Int. Ed.* **2007**, *46*, 7869−7873.

(27) Tanaka, Y.; Saito, S.; Mori, S.; Aratani, N.; Shinokubo, H.; Shibata, N.; Higuchi, Y.; Yoon, Z. S.; Kim, K. S.; Noh, S. B.; Park, J. K.; Kim, D.; Osuka, A. Metalation of Expanded Porphyrins: A Chemical Trigger Used to Produce Molecular Twisting and Möbius Aromaticity. *Angew. Chem., Int. Ed.* **2008**, *47*, 681−684.

(28) Yoneda, T.; Soya, T.; Neya, S.; Osuka, A. [62]Tetradecaphyrin and Its Mono- and Bis-Zn(II) Complexes. *Chem.—Eur. J.* **2016**, *22*, 14518−14522.

(29) Simkowa, I.; Latos-Grażyński, L.; Stępień, M. π Conjugation Transmitted across a d-Electron Metallocene in Ferrocenothiaporphyrin Macrocycles. *Angew. Chem., Int. Ed.* **2010**, *49*, 7665−7669.

(30) Grocka, I.; Latos-Grażyński, L.; Stępień, M. Ruthenocenoporphyrinoids: Conformation Determines Macrocyclic π Conjugation Transmitted Across a d-Electron Metallocene. *Angew. Chem., Int. Ed.* **2013**, *52*, 1044−1048.

(31) Valiev, R. R.; Kurten, T.; Valiulina, L. I.; Ketkov, S. Y.; Cherepanov, V. N.; Dimitrova, M.; Sundholm, D. Magnetically Induced Ring Currents in Metallocenothiaporphyrins. *Phys. Chem. Chem. Phys.* **2022**, *24*, 1666−1674.

(32) Matano, Y. Synthesis of Aza-Oxa-and Thiaporphyrins and Related Compounds. *Chem. Rev.* **2017**, *117*, 3138−3191.

(33) Orłowski, R.; Gryko, D.; Gryko, D. T. Synthesis of Corroles and Their Heteroanalogs. *Chem. Rev.* **2017**, *117*, 3102−3137.

(34) Umasekhar, B.; Shetti, V. S.; Ravikanth, M. Heterocorroles: Corrole Analogues Containing Heteroatom(s) in the Core or at a *meso*-Position. *RSC Adv.* **2018**, *8*, 21100−21132.

(35) Horie, M.; Hayashi, Y.; Yamaguchi, S.; Shinokubo, H. Synthesis of Nickel(II) Azacorroles by Pd-Catalyzed Amination of α,α'-

Dichlorodipyrrin Ni^{II} Complex and Their Properties. *Chem.—Eur. J.* **2012**, *18*, 5919−5923.
(36) Li, S.; Sun, Y.; Li, X.; Smaga, O.; Koniarz, S.; Pawlicki, M.; Chmielewski, P. J. Oxidative Insertion of Amines into Conjugated Macrocycles: Transformation of Antiaromatic Norcorrole into Aromatic Azacorrole. *Chem. Commun.* **2023**, *59*, 3739−3742.
(37) Ito, T.; Hayashi, Y.; Shimizu, S.; Shin, J.-Y.; Kobayashi, N.; Shinokubo, H. Gram-Scale Synthesis of Nickel(II) Norcorrole: The Smallest Antiaromatic Porphyrinoid. *Angew. Chem., Int. Ed.* **2012**, *51*, 8542−8545.
(38) Sakow, D.; Böker, B.; Brandhorst, K.; Burghaus, O.; Bröring, M. 10-Heterocorroles: Ring-Contracted Porphyrinoids with Fine-Tuned Aromatic and Metal-Binding Properties. *Angew. Chem., Int. Ed.* **2013**, *52*, 4912−4915.
(39) Kamiya, H.; Kondo, T.; Sakida, T.; Yamaguchi, S.; Shinokubo, H. *meso*-Thiaporphyrinoids Revisited: Missing of Sulfur by Small Metals. *Chem.—Eur. J.* **2012**, *18*, 16129−16135.
(40) Omori, H.; Hiroto, S.; Takeda, Y.; Fliegl, H.; Minakata, S.; Shinokubo, H. Ni(II) 10-Phosphacorrole: A Porphyrin Analogue Containing Phosphorus at the *Meso* Position. *J. Am. Chem. Soc.* **2019**, *141*, 4800−4805.
(41) Omori, H.; Shinokubo, H. Ni(II) 10-Boracorrole: An Antiaromatic Porphyrinoid Containing a Boron Atom at the *Meso*-Position. *Organometallics* **2019**, *38*, 2878−2882.
(42) Omori, H.; Hiroto, S.; Shinokubo, H. 10-Silacorroles Exhibiting Near-Infrared Absorption and Emission. *Chem.—Eur. J.* **2017**, *23*, 7866−7870.
(43) Ishiyama, T.; Murata, M.; Miyaura, N. Palladium(0)-Catalyzed Cross-Coupling Reaction of Alkoxydiboron with Haloarenes: A Direct Procedure for Arylboronic Esters. *J. Org. Chem.* **1995**, *60*, 7508−7510.
(44) Hitosugi, S.; Nakanishi, W.; Yamasaki, T.; Isobe, H. Bottom-up Synthesis of Finite Models of Helical (n,m)-Single-Wall Carbon Nanotubes. *Nat. Commun.* **2011**, *2*, 492.
(45) Shannon, R. D. Revised Effective Ionic Radii and Systematic Studies of Interatomic Distances in Halides and Chalcogenides. *Acta Crystallogr., Sect. A: Cryst. Phys., Diffr., Theor. Gen. Crystallogr.* **1976**, *32*, 751−767.
(46) Becke, A. D. Density-functional Thermochemistry. III. The Role of Exact Exchange. *J. Chem. Phys.* **1993**, *98*, 5648−5652.
(47) Weigend, F.; Ahlrichs, R. Balanced Basis Sets of Split Valence, Triple Zeta Valence and Quadruple Zeta Valence Quality for H to Rn: Design and Assessment of Accuracy. *Phys. Chem. Chem. Phys.* **2005**, *7*, 3297−3305.
(48) Chen, Z.; Wannere, C. S.; Corminboeuf, C.; Puchta, R.; Schleyer, P. v. R. Nucleus-Independent Chemical Shifts (NICS) as an Aromaticity Criterion. *Chem. Rev.* **2005**, *105*, 3842−3888.
(49) Jusélius, J.; Sundholm, D.; Gauss, J. Calculation of Current Densities Using Gauge-Including Atomic Orbitals. *J. Chem. Phys.* **2004**, *121*, 3952−3963.
(50) Fliegl, H.; Taubert, S.; Lehtonen, O.; Sundholm, D. The Gauge Including Magnetically Induced Current Method. *Phys. Chem. Chem. Phys.* **2011**, *13*, 20500−20518.
(51) Sundholm, D.; Fliegl, H.; Berger, R. J. F. Calculations of Magnetically Induced Current Densities: Theory and Applications. *Wiley Interdiscip. Rev. Comput. Mol. Sci.* **2016**, *6*, 639−678.
(52) Taubert, S.; Sundholm, D.; Jusélius, J. Calculation of Spin-Current Densities Using Gauge-Including Atomic Orbitals. *J. Chem. Phys.* **2011**, *134*, 054123.
(53) Rauhalahti, M.; Taubert, S.; Sundholm, D.; Liégeois, V. Calculations of Current Densities for Neutral and Doubly Charged Persubstituted Benzenes Using Effective Core Potentials. *Phys. Chem. Chem. Phys.* **2017**, *19*, 7124−7131.
(54) Sundholm, D.; Dimitrova, M.; Berger, R. J. F. Current Density and Molecular Magnetic Properties. *Chem. Commun.* **2021**, *57*, 12362−12378.
(55) GIMIC, version 2.2.1; The program can be freely downloaded from https://zenodo.org/records/8183038, 2023.
(56) Oh, J.; Sung, Y. M.; Hong, Y.; Kim, D. Spectroscopic Diagnosis of Excited-State Aromaticity: Capturing Electronic Structures and Conformations upon Aromaticity Reversal. *Acc. Chem. Res.* **2018**, *51*, 1349−1358.
(57) Casida, M. E.; Huix-Rotllant, M. Progress in Time-Dependent Density-Functional Theory. *Annu. Rev. Phys. Chem.* **2012**, *63*, 287−323.
(58) Yanai, T.; Tew, D. P.; Handy, N. C. A New Hybrid Exchange-Correlation Functional Using the Coulomb-Attenuating Method (CAM-B3LYP). *Chem. Phys. Lett.* **2004**, *393*, 51−57.
(59) Reed, A. E.; Curtiss, L. A.; Weinhold, F. Intermolecular Interactions from a Natural Bond Orbital, Donor-Acceptor Viewpoint. *Chem. Rev.* **1988**, *88*, 899−926.

https://doi.org/10.1021/jacs.3c10250
J. Am. Chem. Soc. 2024, 146, 1396−1402